

Dynamical Interactions and Mass Loss Within the Uranian System

STEPHEN R. KANE¹ AND ZHEXING LI¹

¹*Department of Earth and Planetary Sciences, University of California, Riverside, CA 92521, USA*

ABSTRACT

The origin and evolution of planetary rings and moons remains an active area of study, particularly as they relate to the impact history and volatile inventory of the outer solar system. The Uranian system contains a complex system of rings that are coplanar with the highly inclined planetary equator relative to the orbital plane. Uranus also harbors five primary regular moons that play an important role in the distribution of material that surrounds the planet. Here we present the results of a dynamical simulation suite for the Uranian system, intended to explore the interaction between the five primary regular moons and particles within the system. We identify regions of extreme mass loss within 40 planetary radii of Uranus, including eccentricity excitation of particle orbits at resonance locations that can promote moonlet formation within the rings. We calculate a total dynamical particle mass loss rate of 35% within 0.5×10^6 years, and 40% mass loss within 10^7 years. We discuss the implications for post-impact material, including dynamical truncation of stable ring locations, and/or locations of moon formation promoted by dynamical excitation of ring material.

Keywords: planetary systems – planets and satellites: dynamical evolution and stability – planets and satellites: individual (Uranus)

1. INTRODUCTION

The giant planets of the solar system each present opportunities to study the complex interaction between their gravitational influence and the numerous bodies that lie within their Hill spheres. Notable features within each giant planet system, such as rings and moons, provide traceable elements of the dynamical history and angular momentum transfer within those systems, including evidence of past impacts, collisions, and ejections. The numerous particles that exist within the present ring systems of Jupiter (Showalter et al. 1987; Porco et al. 2003), Saturn (Pollack 1975; Porco et al. 2005), Uranus (Elliot et al. 1977; Tyler et al. 1986), and Neptune (Lane et al. 1989; Showalter 2020) are particularly rich sources of dynamical histories within those planetary environments. For example, Saturn’s rings have been studied extensively with respect to their dynamics (Goldreich & Tremaine 1978; Bridges et al. 1984), velocity dispersion (Salo 1995), and the use of density waves to infer fundamental properties of the planetary interior (Hedman & Nicholson

2013; Mankovich et al. 2019; Mankovich & Fuller 2021). Planetary ring material have a variety of sources, including collision events or the desiccation of moons and Kuiper belt objects by tidal forces (Canup 2010; Hyodo et al. 2017; Hyodo & Charnoz 2017). The presence and sustainability of ring material is also an intricate function of the architecture of planetary moons, as well as the intrinsic properties of the planet itself (Petit & Henon 1988; Rubincam 2006; Nakajima et al. 2020; Kane & Li 2022). Furthermore, the vast number of bodies orbiting the solar system outer planets has motivated numerous searches for exomoons (e.g., Hinkel & Kane 2013; Kipping et al. 2013; Heller et al. 2014; Hill et al. 2018) and rings (e.g., Arnold & Schneider 2004; Kenworthy & Mamajek 2015; Zuluaga et al. 2015; Sucerquia et al. 2020). The solar system giant planets and their associated companions can serve as important analogs for compact exoplanetary systems, revealing insight into their formation and architectures (Kane et al. 2013; Makarov et al. 2018; Dobos et al. 2019; Batygin & Morbidelli 2020).

Ice giant planets are of particular interest with respect to their dynamical environment since they have played a significant role in planet formation and evolution at the outer edges of the protoplanetary disk

(Ford & Chiang 2007; Dawson & Murray-Clay 2012). The Neptunian system may be atypical of ice giant moon systems given the relatively rare capture scenario for its major moon, Triton (Agnor & Hamilton 2006; Li & Christou 2020; Li et al. 2020). The Uranian system is especially diverse with respect to its dynamical history and system of moons and rings, providing a valuable template from which to explore the development of ice giant architectures (Peale 1999; Esposito 2002; Jacobson 2014). The Uranian moons continue to be the target of observations that aim to update their orbital ephemerides and study their compositions (Brozović & Jacobson 2022; Paradis et al. 2023). Uranus has five primary regular moons, all of which lie within 25 planetary radii of the planet and exhibit a myriad of geological features (Camargo et al. 2022; Kirchoff et al. 2022; Castillo-Rogez et al. 2023). The dynamical state of the moon system has also been studied in detail (Dermott et al. 1988; Ćuk et al. 2020), including long-term stability issues and collision scenarios (Ćuk et al. 2022), tidal evolution (Tittlemore & Wisdom 1988, 1989, 1990), and resonances (Lazzaro et al. 1984; Quillen & French 2014; French et al. 2015; Charalambous et al. 2022). The Uranian system contains substantial evidence of a rich impact history. The most compelling evidence is contained within Uranus itself, whose large axial tilt origin has been explained via various mechanisms (Boué & Laskar 2010; Lu & Laughlin 2022; Saillenfest et al. 2022), and frequently attributed to a giant impactor early in its history (Korycansky et al. 1990; Slattery et al. 1992; Kegerreis et al. 2018). Such evidence is also contained upon the moon surfaces, exhibiting a vast range of geological and topographical features (Johnson et al. 1987b,a). Indeed, the formation and subsequent evolution of the moons may be attributed to a giant impact event (Izidoro et al. 2015; Ida et al. 2020; Chau et al. 2021; Salmon & Canup 2022; Woo et al. 2022), and is consistent with the moon’s prograde motion and relative orbital coplanarity with the planet’s equatorial plane (Morbidelli et al. 2012). Uranus also has a significant ring system which, when including the relatively tenuous outer ring system (Showalter & Lissauer 2006), extends to four planetary radii and well beyond the fluid body Roche limit. The Uranian rings have long been a discussion topic regarding their formation and sustainability (Goldreich & Tremaine 1979; Esposito & Colwell 1989), and suggested as a probe of the planetary interior via ring seismology (A’Hearn et al. 2022). The rings also possess a complex relationship with the moons, notably with accretion processes and moonlets within the Roche

limit (Canup & Esposito 1995), and the kinematics of shepherding interactions between the moons and rings (Goldreich & Porco 1987; Porco & Goldreich 1987). An exploration of the concise dynamical influence of the moons over the distribution of past and present material within the Uranian system will provide further insight into the evolution of this fascinating system of moons and rings.

Here, we present the results of a detailed dynamical analysis for the five primary regular moons in the Uranian system, and their influence on injected particles into the system. The results show the dynamical exclusion regions and ring material mass loss rates around Uranus for timescales of up to 10^7 years. Section 2 describes the architecture of the Uranian ring and moon system, with comparison to those of Jupiter and Saturn. Section 3 provides a description of the dynamical simulation methodology and the results for the moons and injected particles. The simulation results and their implication for moon and ring evolution are discussed in Section 4. Concluding remarks and suggestions for additional work are provided in Section 5.

2. ARCHITECTURE OF THE URANIAN SYSTEM

Amongst the known population of moons, regular moons of giant planets are particularly notable in that they likely formed either with the planet or via subsequent collision events (Lunine & Stevenson 1982; Canup & Ward 2002, 2006; Ronnet & Johansen 2020), as evidenced by their typically equatorial prograde orbits, and are often large enough to exhibit hydrostatic equilibrium, resulting in a near-round morphology. At the time of writing, the Uranus system is known to harbor a total of 27 moons, including the five major regular moons of (in order of increasing semi-major axis) Miranda, Ariel, Umbriel, Titania, and Oberon¹. The smallest of these moons, Miranda, has a mean radius of ~ 235 kms, placing it near the limit of hydrostatic equilibrium (Thomas 1988; Beddingfield et al. 2015). Even so, Miranda is almost seven times more massive than the combined mass of the smaller moons within the system. Miranda, in turn, is ~ 20 times less massive than the next largest moon, Ariel. This demonstrates the clear gravitational dominance of the five primary moons, and the relatively small influence of Miranda compared with the other four.

Shown in Figure 1 is a scaled view of the moon systems for Jupiter (top), Saturn (middle), and Uranus (bottom), where the separations from the planetary centers are in units of the host planet radius. The regular moons

¹ <https://solarsystem.nasa.gov/moons/overview/>

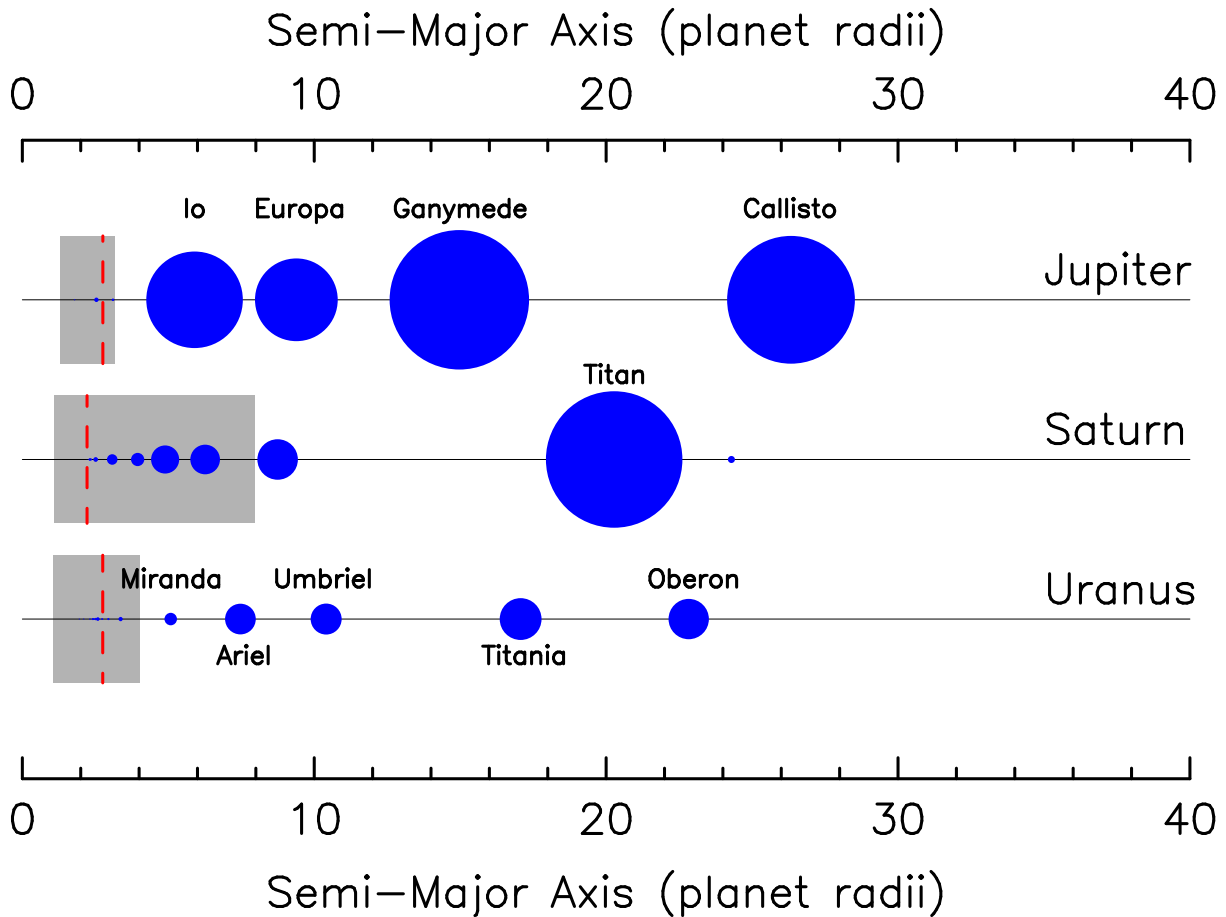


Figure 1. The regular moons and rings of the Jupiter (top), Saturn (middle), and Uranus (bottom) systems. The relative sizes of the moons are shown, and their semi-major axes are provided in units of the host planet radii. The extent of the current ring systems, including dense and tenuous rings, are shown as gray regions, and the vertical red dashed lines indicate the location of the fluid satellite Roche limit for each planet.

(larger moons that likely formed in orbit of the planet) within each system are shown in blue and their sizes are scaled relative to each other. The location of the fluid satellite Roche limits (red dashed lines) are 2.76, 2.22, and 2.75 planetary radii for Jupiter, Saturn, and Uranus, respectively. Also shown are the extent of the ring systems for each planet (gray regions). Note that the shaded ring regions incorporate both dense and tenuous rings, including faint outer ring systems. For example, the indicated ring region for Jupiter extends to the Thebe gossamer ring (3.16 Jupiter radii), and the D–E rings are included for Saturn, extending to 7.96 Saturn radii. In the case of Uranus, the faint μ and ν rings, discovered using observations by the Hubble Space Telescope (HST) (Showalter & Lissauer 2006) extend out to 4.03 Uranus radii.

Although there are significant differences in the size distribution and architectures of the three planet/moon systems represented in Figure 1, there are also numerous similarities. All three planets harbor their regular

moons within 30 planetary radii of their host planet, and within 1/25 of their respective Hill radii. The sizes and masses of the largest Uranian moons with respect to Uranus are roughly proportional to the relative sizes and masses of the Galilean moons compared with Jupiter, consistent with a scaling of moon formation with the mass of the primary planet (Canup & Ward 2006). In addition to the gravitational effect of the orbiting moons on material surrounding the planet (Petit & Henon 1988; Nakajima et al. 2020), such as the Laplace resonance effects of the Galilean moons (Malhotra 1991; Peale & Lee 2002; Kane & Li 2022), there are various other factors at work that both contribute to and remove such material (Daisaka et al. 2001). Additions to material may originate from impacts and degassing events on moons (Esposito 2002). Beyond the Roche limit, material will often accrete to form new moons, such as some of those moons that are currently present within Saturn’s ring structure (Charnoz et al. 2010; Crida & Charnoz 2012; Salmon & Canup 2017).

Removal of ring material may involve several non-gravitational effects, particularly for tenuous rings that are more susceptible to such processes as Poynting-Robertson drag, the Yarkovsky effect, and those related to planetary magnetospheres (Burns et al. 1999; Rubincam 2006; Kobayashi et al. 2009). The dynamical simulations described in this work focus on dense material that is more likely to be influenced by the gravitational and accretion effects imposed by the planet and moons in the system.

3. DYNAMICAL SIMULATIONS

This section describes the dynamical simulations, their configuration, results for the five major moons, and particle injections.

3.1. *Dynamics of the Uranian Moons*

The dynamical evolution of the Uranus moons have previously been studied in detail (Greenberg 1975a,b; Lainey 2008), including their resonances and the consequences for their tidal development (Ćuk et al. 2020; Charalambous et al. 2022). Our simulations explore the dynamical influence of the five main regular moons of Uranus since, as described in Section 2, even the smallest of these moons (Miranda) is substantially more massive than the combined mass of the smaller moons, and so these five major moons dominate the gravitational perturbations within the Uranian Hill sphere. Therefore, we commenced our dynamical analysis by examining the orbital stability of the major moons over 1–10 million year timescales. The purpose of these initial simulations were to establish a baseline performance of our methodology and examine the eccentricity variations of the major moons.

Our simulations were conducted using the REBOUND N-body integrator package (Rein & Liu 2012) that applies the symplectic integrator WHFast (Rein & Tamayo 2015). The initial conditions and orbital elements of the Uranian moon system were extracted from the Jet Propulsion Laboratory (JPL) Planetary and Lunar Ephemerides DE440 and DE441 (Park et al. 2021). These data were cross-referenced with those provided by Scott Sheppard². The simulations do not incorporate the 2.3% oblateness of Uranus (Helled et al. 2010), compared with the 6.5% oblateness of Jupiter (Buccino et al. 2020), nor do they include the effects of tidal dissipation. Note that the moon system stability has previously been verified for non-MMR-crossing conditions (e.g., Dermott & Nicholson 1986; Laskar 1986; Malhotra et al. 1989; Lazzaro 1991).

The resulting predicted eccentricity evolution of the moons over a period of 10^6 years are shown in Figure 2. Over the timescale shown, the orbits of the moons are remarkably stable, with eccentricity variations generally remaining below 0.005. The exception to this is the eccentricity of Miranda, which regularly rises above 0.005 and exhibits several modes of variability frequency. A Fourier analysis of the eccentricity data for Miranda reveals a high frequency variation with a period of ~ 475 years, similar to the other major moons, in addition to a low frequency eccentricity variation with a period of $\sim 20,470$ years. These high frequency results are consistent with those of Malhotra et al. (1989), whereas the duration of their integration was not sensitive to the low frequency variations found in our data. However, there are some important caveats to note regarding the orbital evolution of the system. Mean motion resonances (MMR) play a critical role in the evolution of the orbits, as they are relatively efficient in transferring angular momentum between bodies that can lead to eccentricity increases and tidal effects. Although none of the major moons are currently in MMR with each other, recent simulations have demonstrated a past Ariel–Umbriel 5:3 MMR and Miranda–Umbriel 5:3 MMR (Titemore & Wisdom 1990; Ćuk et al. 2020). Such resonances may have had a particularly profound effect on both the orbit and geology of Miranda (Hammond & Barr 2014; Beddingfield et al. 2015, 2022), whereby inclination and eccentricity excitation of Miranda’s orbit resulted in significant tidal heating of the moon (Dermott et al. 1988; Ćuk et al. 2020). Furthermore, the dynamical simulations performed by Ćuk et al. (2020) reveal the potential for an Ariel–Umbriel 5:3 MMR crossing event beyond 10^7 years that excites the eccentricity of Miranda to ~ 0.03 . Thus, MMR events will continue to play a role in the evolution of the Uranian moon system. Indeed, locations of MMR will be a crucial factor in understanding the effect of the major moons on other material that lies within the Uranian system, as described in Section 3.2.

3.2. *Gravitational Influence of the Major Moons*

To investigate the gravitational influence of the major moons on particles within the system, most particularly material that may potentially participate in the formation of rings or moonlets, we conducted an extended series of dynamical simulations. These simulations utilized the same REBOUND framework described in Section 3.1 and introduced particles into the system. We adopted particle densities equivalent to water ice (0.917 g/cm^3), and spherical radii of ~ 1 meter, yielding a particle mass of ~ 3841 kg. The particles were

² <https://sites.google.com/carnegiescience.edu/sheppard/>

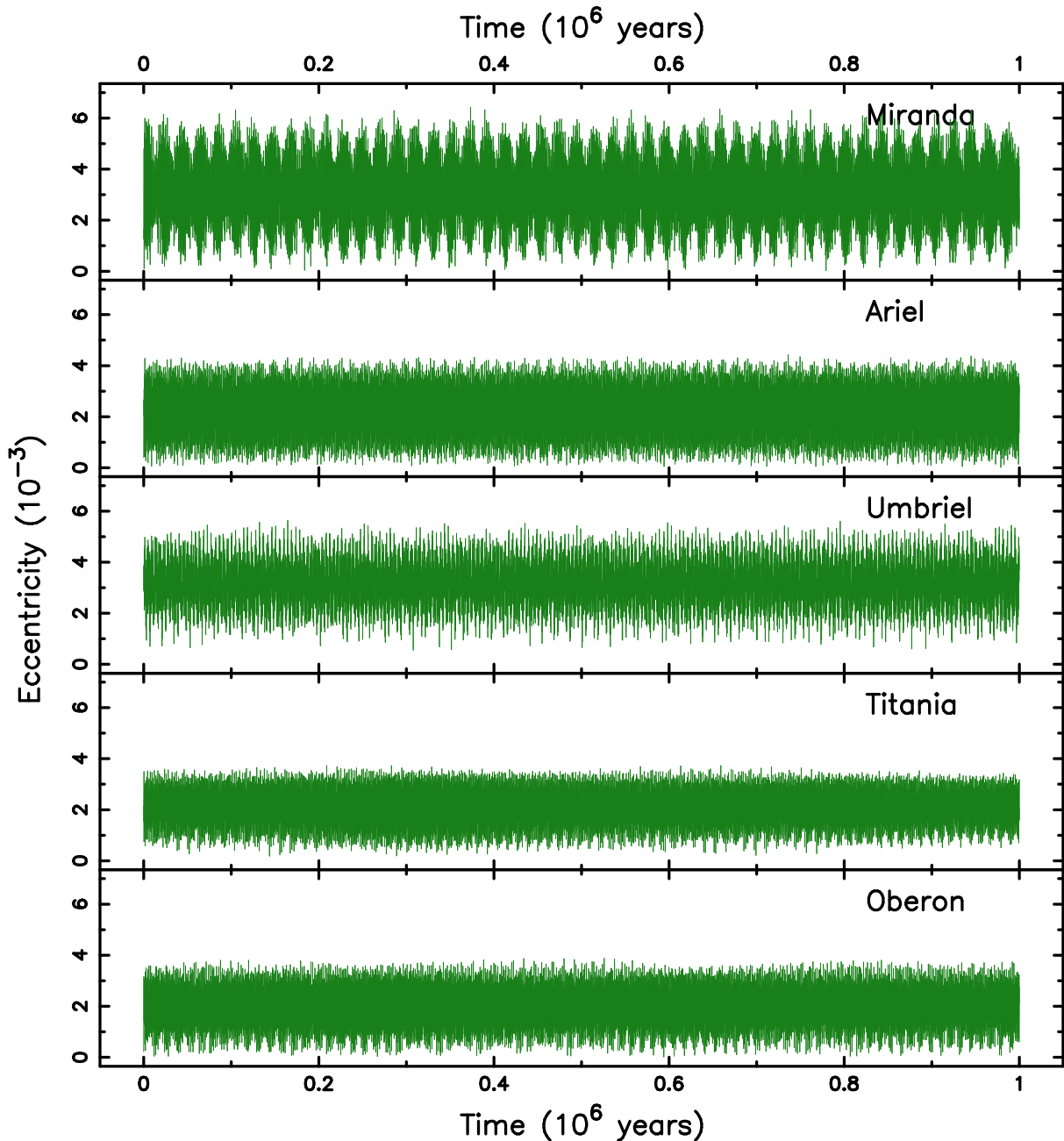


Figure 2. Eccentricity as a function of time for the Uranus major moons of Miranda, Ariel, Umbriel, Titania, and Oberon. The eccentricity values were recorded every 100 years during a 10^6 year simulation, as described in Section 3.

injected into circular orbits that are coplanar with the Uranus equator. The particles were injected into 1000 evenly spaced semi-major axis locations between 1 and 40 planetary radii, resulting in a distance resolution of ~ 1000 kms. The inner boundary for the semi-axis range was chosen to ensure that our simulations explore the region interior to the fluid satellite Roche limit of Uranus, which is ~ 2.75 planetary radii (see Section 2). The outer boundary of 40 planetary radii was chosen in the context of the planet–moon separations shown in Figure 1. The

Hill radius of Uranus is immense (more than 2600 planetary radii) due to its relatively large semi-major axis, but 40 planetary radii sufficiently captures the extent of the major moons. The duration of each simulation was 10^7 years, which translates to 1.2×10^8 orbits at the outer boundary of our chosen semi-major axis range. In order to adequately sample the dynamical interactions within the system, the time step for the simulations was 0.05 of the orbital period of Miranda, except for locations interior to Miranda’s orbit where the time step

was 0.05 of the particle orbital period. The evolution of the orbital parameters for all objects within the system were output every 100 years to allow analysis of individual orbital elements, such as the eccentricity evolution of the major moons described in Section 3.1. The survival of the injected particles at each location were evaluated based on the fraction of the simulation time for which they remained in orbit within the system. Removal from the system could result from either ejection from the Uranus gravity well or collision with one of the other bodies included in the simulation.

The results of the simulations are summarized in the plots shown in Figure 3. The top two panels show green lines that represent the survival time of the injected particles (as a percentage of the total simulation time) as a function of semi-major axis (in units of planetary radii). The results after 10^6 years and 10^7 years and shown in the top and middle panels, respectively. The vertical dotted lines indicate the locations of the major moons, and the vertical dashed lines represent the locations of the rigid and fluid body Roche limits for Uranus. A comparison of the top and middle panels show that much of the particle loss has transpired by 10^6 years. The peaks at each of the moon locations is evidence of their ability to harbor trojan bodies within their orbit. The exception to this are Titania and Oberon, the most massive of the moons, whose orbits are largely cleared by the time 10^7 years has elapsed, though Trojan bodies may remain. Of particular note is the relatively large gap in simulation survival for the injected particles within the range 15–25 Uranus radii. It is also worth noting that the inner boundary of dynamical stability is primarily located at 4.24 Uranus radii for the 10^7 year simulation, which is just slightly exterior to the extent of the ν ring (see Section 2). Therefore, the dynamical constraints imposed by the major moons allow for an age of the Uranus rings that is larger than 10^7 years, though there are numerous non-gravitational forces that can limit the lifetime of such structures (Burns et al. 1979).

As described in Section 3.1, a major contributor to the dynamics of the system are the locations of MMR caused by the gravitational influence of the major moons. Table 1 provided the semi-major axis, a , and the important MMR locations for each of the major moons in units of Uranus radii. For example, the 10^7 year simulation shows a line of instability located 3.59 Uranus radii, which corresponds to the location of the 3:1 MMR with Ariel, and creates a dynamically unstable region within the ring structure. In contrast, a spike of stability is present at 10^7 years located at 20.1 Uranus radii. Ac-

ording to Table 1, this does not correspond to a location of MMR, but rather is surrounded by other regions of MMR caused by the moons Umbriel, Titania, and Oberon. As one final example, a location of instability is apparent in both the 10^6 year and 10^7 year simulations results at 13.02 Uranus radii, which corresponds to the 3:2 MMR with Titania and closely aligns with the 5:7 MMR with Umbriel.

Even when injected particles are not lost from the system, the gravitational influence of the moons may still manifest by altering the orbits of the particles. The bottom panel of Figure 3 shows the change in eccentricity, δe , that occurs for each particle at the end of the 10^7 year simulation. For example, the top and middle panels of Figure 3 indicate a complicated structure of Titania and Oberon MMR locations between 25–29 Uranus radii, beyond which the gravitational perturbation effects cease to have a significant impact on simulation survival rates. However, the bottom panel of Figure 3 reveals that the extensive MMR locations beyond 29 Uranus radii (see Table 1) result in the excitation of particles into eccentric orbits. For example, the location of the 3:7 MMR with Titania and 2:3 MMR with Oberon combine to cause a significant region of higher eccentricity at ~ 30 Uranus radii. Furthermore, the locations of 3:1 and 5:2 MMR with Ariel excite particles between 3–4 Uranus radii. For such small separations from the giant planet, tidal dissipation and circularization become important long-term effects (Ogilvie 2014), especially as particles beyond the Roche limit accrete into moonlets (see Section 4). Since tidal dissipation is not included in our simulations, the eccentricities shown in the bottom panel of Figure 3 may be considered upper limits on the perturbative effects of the moons on the injected particles. It should further be noted that MMR locations in isolation do not intrinsically result in instability, but rather the overlap of nonlinear secular resonances can serve as a driver for secular chaos (Lithwick & Wu 2011). Thus, it is the complex combination of the Uranian moon MMR locations that produce much of the observed mass loss within the system.

To further explore the nature of the gravitational perturbations taking place close to the planet, we performed an additional 10^7 year simulation at higher resolution within the semi-major axis range 1–5 planetary radii. As for the previous simulations, we used 1000 evenly spaced semi-major axis locations which, in this case, produced a distance resolution of ~ 100 kms. The results of this simulation are shown in Figure 4 where, in addition to the features of Figure 3, we include black vertical dotted lines to indicate the MMR locations of greatest influence within the 1–5 planetary radii range. The increased res-

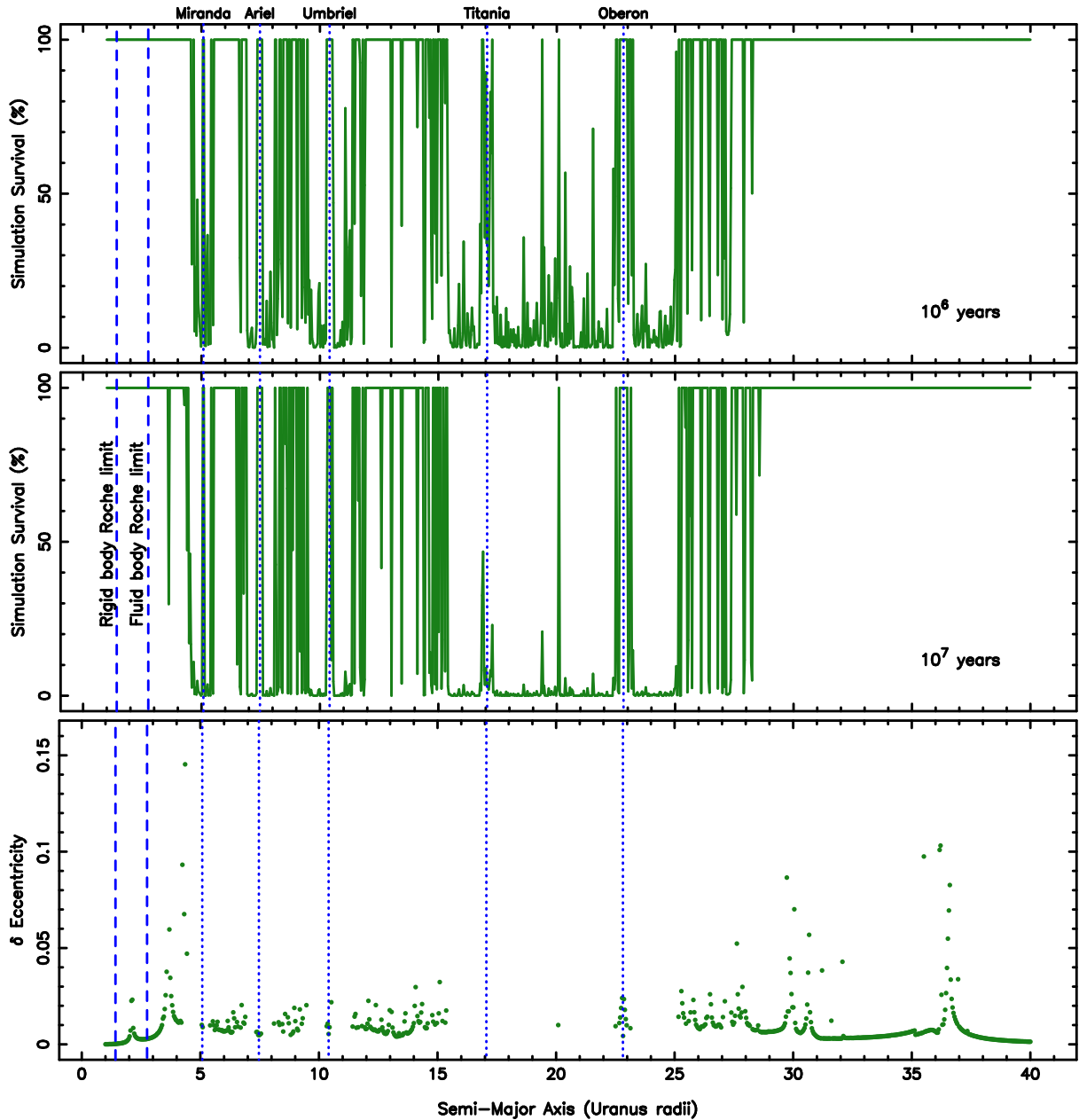


Figure 3. Results of the particle injection and survival for the dynamical simulations, showing the outcome after 10^6 years (top panel) and 10^7 years (middle panel). The horizontal axis is the separation from Uranus in planetary radii, and the vertical axis shows the percentage of the total dynamical simulation that particles survived at that location, represented by the green line. The vertical dotted lines represent the semi-major axes of the major moons, and the vertical dashed lines represent the locations of the rigid and fluid Roche limits. The bottom panel shows the change in eccentricity that occurs for each particle as a function of their initial semi-major axis during the course of the 10^7 year simulations.

olution of this simulation reveals important resonance features, including the previously noted 3:1 MMR with Ariel. In particular, the effects of the 7:3 MMR with Ariel and the 3:2 MMR with Miranda are clearly visible, as well as the coincident location of the 7:5 MMR with Miranda and 5:2 MMR with Ariel. The primary MMR within the region interior to Miranda is the 2:1

MMR with Ariel, whose presence (combined with the 3:1 MMR with Umbriel) plays a major role in clearing material between 4.5 and 5 planetary radii.

As pointed out earlier, the comparison of the top and middle panels of Figure 3 indicate that most of the mass loss occurred within the initial 10^6 year time frame. We investigated the mass loss rate by calculating the per-

Table 1. Mean motion resonance locations for Uranus moons.

Moon	a	3:1	5:2	7:3	2:1	3:2	7:5	5:7	2:3	1:2	3:7	2:5	1:3
Miranda	5.062	2.43	2.75	2.88	3.19	3.86	4.05	6.34	6.63	8.04	8.91	9.33	10.53
Ariel	7.474	3.59	4.06	4.25	4.71	5.70	5.97	9.35	9.79	11.86	13.15	13.77	15.55
Umbriel	10.419	5.01	5.66	5.92	6.56	7.95	8.33	13.04	13.65	16.54	18.33	19.19	21.67
Titania	17.055	8.20	9.26	9.69	10.74	13.02	13.63	21.34	22.35	27.07	30.00	31.42	35.48
Oberon	22.830	10.98	12.39	12.98	14.38	17.42	18.24	28.57	29.92	36.24	40.16	42.05	47.49

NOTE—All distances are in units of Uranus radii.

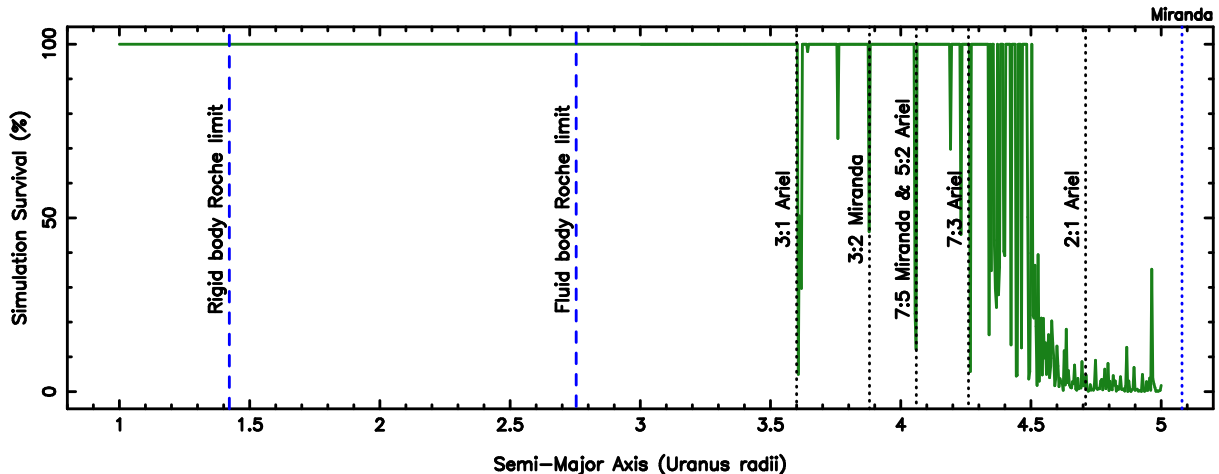


Figure 4. Results of the 10^7 year particle injection at higher resolution in the semi-major axis range of 1–5 Uranus radii. As for the top two panels of Figure 3, the green line represents the percentage survival of the injected particle, the vertical dashed lines represent the Roche limit locations, and the blue vertical dotted line represents the semi-major axis of Miranda. The black vertical dotted lines indicate the locations of some MMR locations, corresponding to those values provided in Table 1.

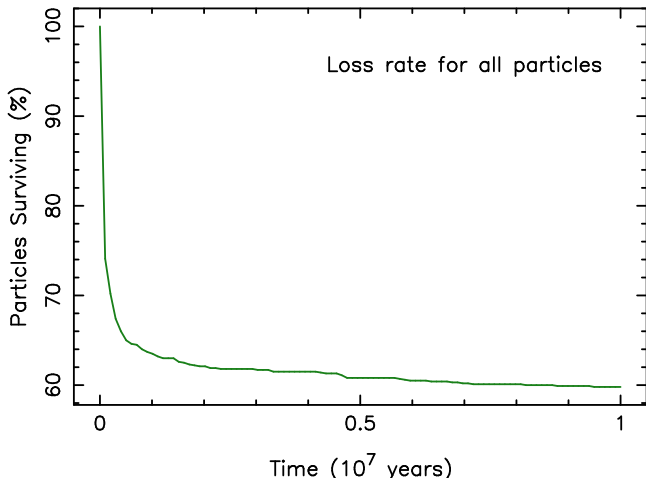


Figure 5. Loss rate for the injected particles into the Uranus system, shown as a function of time (fractions of 10^7 years) and the percentage of particles that survive.

centage of particles surviving throughout the full 10^7

year simulation, the results of which are shown in Figure 5. These calculations reveal the dramatic decline in the injected material into the system, showing that 35% of the total number of particles are lost within the first 0.5×10^6 years of the simulation. Subsequent mass loss rates are far more gradual, with an additional $\sim 5\%$ mass loss over the following $\sim 10^7$ years. Thus, once the full simulation time of 10^7 is reached, $\sim 40\%$ of the injected mass has been lost. Therefore, there is a $\sim 13\%$ difference between the remaining particle mass represented in the top two panels of Figure 3. The mass loss rates described here demonstrate the rapid sculpting of material that occurs due to the gravitational influence of the major moons orbiting Uranus, and that any rings that form in the affected regions shown in Figure 3 are relatively short-lived.

4. DISCUSSION

The giant planets of the solar system have greatly influenced the architecture and evolution of the inner so-

lar system, as well as the distribution of material and minor bodies out into the Kuiper belt (Laskar 1988; Deienno et al. 2011; Dawson & Murray-Clay 2012; Deienno et al. 2014; Horner et al. 2020a; Clement et al. 2021; Vervoort et al. 2022; Kane 2023). A consequence of these interactions are the occurrence rate of impacts that can be the source of material that remains distributed within the Hill radius of the planet. Such material may be sourced from minor bodies or moons that move within the Roche limit of the planet (Canup & Esposito 1995; Hyodo et al. 2017; Hyodo & Charnoz 2017), from impactors on the moons within the system (Plescia & Boyce 1985; Zahnle et al. 2003; Kirchoff & Schenk 2010; Hueso et al. 2018; Ferguson et al. 2020), or even moon collisions (Barbara & Esposito 2002; French & Showalter 2012). As described in Section 1, impacts have played a profound role in the evolution of Uranus, both intrinsically and to its dynamical environment (Parisi 2011; Reinhardt et al. 2020), and may have been a source for building the major moons of the Uranus system (Salmon & Canup 2022).

As described in Section 1, the ring system of Uranus is both fascinating and complex (Goldreich & Tremaine 1979; Esposito & Colwell 1989; Showalter & Lissauer 2006; A’Hearn et al. 2022), and whose evolution is likely connected to the simultaneous evolution of the moons within the system (Goldreich & Porco 1987; Porco & Goldreich 1987; Canup & Esposito 1995). Section 2 discusses the size of the Uranian ring system, where tenuous rings extend beyond the fluid Roche limit to ~ 4 Uranus radii. Contributions to the ring material may include collision events, grinding down of small moons, and outgassing from the major moons (Esposito 2002). Sustaining ring material within the gravitational influence of the planet is subject to a variety of loss processes, of which the dynamical effects caused by the major moons are herein presented. The results of our simulations provided in Section 3.2 show the important consequence of these dynamical effects on the sustainability of material within the system, and the critical role of MMR locations in this context. Gravitational dessiccation of ring material interior to the orbit of Miranda is dominated by the Miranda and Ariel MMR locations, with a particularly severe truncation of stable ring orbits occurring beyond ~ 4.3 Uranus radii in the vicinity of Miranda and within the 2:1 MMR with Ariel. Ringlets are sustainable in the gaps between moons out as far as Titania, although such ring material would likely require being sourced via a substantial impact or primordial formation material. Our mass loss simulations show that the vast majority of coplanar material is

lost within a million years of orbital insertion, restricting and sculpting the range of possible ring architectures for the system. The mass loss caused by the major moons may have been further exacerbated by previous orbital configurations if MMR crossing events between moons did indeed occur (Titemore & Wisdom 1990; Ćuk et al. 2020).

Beyond the dynamical loss processes caused by the major moons described in this work, there are numerous other factors that can desiccate material within the system, such as Poynting-Robertson drag and the Yarkovsky effect (Rubincam 2006; Kobayashi et al. 2009). However, many of these non-gravitational forces act upon material that is significantly smaller than that considered in our simulations (Burns et al. 1979). The bottom panel of Figure 3 demonstrates the excitation of orbital eccentricities for particles near locations of MMR. Such excitation beyond the Roche limit can promote collisions and the accretion of material into moonlets. Moonlet formation represents another means of mass loss from the total distribution of orbiting particles, and can occur on timescales that are comparable to the simulations described in this work (Crida & Charnoz 2012). Another caveat to our methodology that is worth noting is the ejection of particles into the equatorial plane of the planet, particularly given the high axial tilt of the planet relative to the orbital plane. Although the distribution of impactor trajectories is unlikely to be isotropic, neither will they necessarily be aligned with the present tilt of the Uranian rotational axis. However, orbital precession of material that originates from moon impacts or moon-moon collisions will result in an eventual collapse of the material into the planet’s equatorial plane, where they will be subjected to the gravitational influences described in this work. The high obliquity of Uranus does result in greater exposure of the ring surface area to the solar wind (Curtis & Ness 1985). The effects of such exposure are largely mitigated by the Uranus magnetic field (Connerney et al. 1987; Stanley & Bloxham 2006), whose maximum strength occurs at ~ 4.2 Uranus radii, slightly beyond the extent of the rings, and whose magnetopause boundary occurs at ~ 18.0 Uranus radii, slightly beyond the orbit of Titania (Ness et al. 1986).

5. CONCLUSIONS

The formation and evolution of the solar system giant planets and their local environments is an extraordinarily complex research area, with a vast number of associated interacting bodies. Each giant planet system has a different story to tell, a story that is largely informed by the properties of the planet (interior, atmosphere, orbit,

spin angular momentum), moons (composition, craters, geology, orbit), and rings (composition, density, sustainability). The case of Uranus is of particular interest since it has significant divergence in many of these properties from its sibling giant planets, leading to investigations on how aspects such as the high obliquity, ring structure, and moon geology may be related to each other. A major step in tracing such connections and their evolution is the concise evaluation of the processes that are contributing and removing material from the system that may yield insight into the plethora of processes acting upon the material and their sources.

The simulation results presented here explore the specific component of dynamical interactions within the Uranian system and their contribution to mass loss processes. The five major moons of Uranus are the major perturbative agents, and have proceeded through their own complicated interactions including periods of MMR with each other. Assuming dense material such as that described in Section 3.2, our results predict a 35% mass loss of material, evenly distributed between 0–40 Uranus radii, within the relatively small timeframe of 0.5×10^6 years. The vast majority of the mass loss occurs within the semi-major axis range of 15–25 Uranus radii, where the perturbations are largely caused by the major MMR locations with the two most massive moons of Titania and Oberon. Their larger orbital distances from Uranus also enable them to have larger Hill radii, further increasing their perturbative influence over the injected particles. An additional region of mass loss worth highlighting is that interior to the orbit of Miranda, where the present ring system lies. The MMR locations resulting from Miranda and Ariel dominate the mass loss within this region, and past MMR crossings may have enhanced this mass loss effect. These regions of significant particle loss can greatly truncate the sustainability of rings or moonlet formation within the system.

The dynamical results presented here may be combined with moon formation processes, the effects of orbital migration within an accretion disk, and the non-gravitational forces acting upon the injected material. However, a thorough analysis of the dynamics within the Uranian system requires further data that is currently unavailable for the planet and its moons. The interior structure of the planet, its complex magnetic field, and the diverse geology of the moons, all form the basis of key scientific questions that would be primarily addressed via in-situ measurements from a Uranus orbiter mission (Arridge et al. 2012, 2014; Fletcher et al. 2020b,a; Blanc et al. 2021; Cartwright et al. 2021; Fletcher et al. 2022). Furthermore, although their detection remains challenging with most current detection techniques (Kane 2011), ice giant analogs in exoplanetary systems will aid in addressing these questions (Wakeford & Dalba 2020). Overcoming the detection challenges will provide a vast inventory of planets from which statistical studies of occurrence rates, dynamical properties, and formation scenarios for ice giant planets may be inferred. The increasing consolidation of data from solar system and exoplanetary science will continue to unveil the properties of ice giants (Horner et al. 2020b; Kane et al. 2021), and allow a deeper exploration of their dynamical histories.

ACKNOWLEDGEMENTS

The authors would like to thank the anonymous referees for their useful contributions and feedback that improved the manuscript. The results reported herein benefited from collaborations and/or information exchange within NASA’s Nexus for Exoplanet System Science (NExSS) research coordination network sponsored by NASA’s Science Mission Directorate.

Software: REBOUND (Rein & Liu 2012)

REFERENCES

- Agnor, C. B., & Hamilton, D. P. 2006, *Nature*, 441, 192, doi: [10.1038/nature04792](https://doi.org/10.1038/nature04792)
- A’Hearn, J. A., Hedman, M. M., Mankovich, C. R., Aramona, H., & Marley, M. S. 2022, *PSJ*, 3, 194, doi: [10.3847/PSJ/ac82bb](https://doi.org/10.3847/PSJ/ac82bb)
- Arnold, L., & Schneider, J. 2004, *A&A*, 420, 1153, doi: [10.1051/0004-6361:20035720](https://doi.org/10.1051/0004-6361:20035720)
- Arridge, C. S., Agnor, C. B., André, N., et al. 2012, *Experimental Astronomy*, 33, 753, doi: [10.1007/s10686-011-9251-4](https://doi.org/10.1007/s10686-011-9251-4)
- Arridge, C. S., Achilleos, N., Agarwal, J., et al. 2014, *Planet. Space Sci.*, 104, 122, doi: [10.1016/j.pss.2014.08.009](https://doi.org/10.1016/j.pss.2014.08.009)
- Barbara, J. M., & Esposito, L. W. 2002, *Icarus*, 160, 161, doi: [10.1006/icar.2002.6962](https://doi.org/10.1006/icar.2002.6962)
- Batygin, K., & Morbidelli, A. 2020, *ApJ*, 894, 143, doi: [10.3847/1538-4357/ab8937](https://doi.org/10.3847/1538-4357/ab8937)
- Beddingfield, C. B., Burr, D. M., & Emery, J. P. 2015, *Icarus*, 247, 35, doi: [10.1016/j.icarus.2014.09.048](https://doi.org/10.1016/j.icarus.2014.09.048)
- Beddingfield, C. B., Leonard, E., Cartwright, R. J., Elder, C., & Nordheim, T. A. 2022, *PSJ*, 3, 174, doi: [10.3847/PSJ/ac7be5](https://doi.org/10.3847/PSJ/ac7be5)

- Blanc, M., Mandt, K., Mousis, O., et al. 2021, *SSRv*, 217, 3, doi: [10.1007/s11214-020-00769-5](https://doi.org/10.1007/s11214-020-00769-5)
- Boué, G., & Laskar, J. 2010, *ApJL*, 712, L44, doi: [10.1088/2041-8205/712/1/L44](https://doi.org/10.1088/2041-8205/712/1/L44)
- Bridges, F. G., Hatzes, A., & Lin, D. N. C. 1984, *Nature*, 309, 333, doi: [10.1038/309333a0](https://doi.org/10.1038/309333a0)
- Brozović, M., & Jacobson, R. A. 2022, *AJ*, 163, 241, doi: [10.3847/1538-3881/ac617f](https://doi.org/10.3847/1538-3881/ac617f)
- Buccino, D. R., Helled, R., Parisi, M., Hubbard, W. B., & Folkner, W. M. 2020, *Journal of Geophysical Research (Planets)*, 125, e06354, doi: [10.1029/2019JE006354](https://doi.org/10.1029/2019JE006354)
- Burns, J. A., Lamy, P. L., & Soter, S. 1979, *Icarus*, 40, 1, doi: [10.1016/0019-1035\(79\)90050-2](https://doi.org/10.1016/0019-1035(79)90050-2)
- Burns, J. A., Showalter, M. R., Hamilton, D. P., et al. 1999, *Science*, 284, 1146, doi: [10.1126/science.284.5417.1146](https://doi.org/10.1126/science.284.5417.1146)
- Camargo, J. I. B., Veiga, C. H., Vieira-Martins, R., Fienga, A., & Assafin, M. 2022, *Planet. Space Sci.*, 210, 105376, doi: [10.1016/j.pss.2021.105376](https://doi.org/10.1016/j.pss.2021.105376)
- Canup, R. M. 2010, *Nature*, 468, 943, doi: [10.1038/nature09661](https://doi.org/10.1038/nature09661)
- Canup, R. M., & Esposito, L. W. 1995, *Icarus*, 113, 331, doi: [10.1006/icar.1995.1026](https://doi.org/10.1006/icar.1995.1026)
- Canup, R. M., & Ward, W. R. 2002, *AJ*, 124, 3404, doi: [10.1086/344684](https://doi.org/10.1086/344684)
- . 2006, *Nature*, 441, 834, doi: [10.1038/nature04860](https://doi.org/10.1038/nature04860)
- Cartwright, R. J., Beddingfield, C. B., Nordheim, T. A., et al. 2021, *PSJ*, 2, 120, doi: [10.3847/PSJ/abfe12](https://doi.org/10.3847/PSJ/abfe12)
- Castillo-Rogez, J., Weiss, B., Beddingfield, C., et al. 2023, *Journal of Geophysical Research (Planets)*, 128, e2022JE007432, doi: [10.1029/2022JE007432](https://doi.org/10.1029/2022JE007432)
- Charalambous, C., Giuppone, C. A., & Guilera, O. M. 2022, *Ap&SS*, 367, 54, doi: [10.1007/s10509-022-04083-0](https://doi.org/10.1007/s10509-022-04083-0)
- Charnoz, S., Salmon, J., & Crida, A. 2010, *Nature*, 465, 752, doi: [10.1038/nature09096](https://doi.org/10.1038/nature09096)
- Chau, A., Reinhardt, C., Izidoro, A., Stadel, J., & Helled, R. 2021, *MNRAS*, 502, 1647, doi: [10.1093/mnras/staa4021](https://doi.org/10.1093/mnras/staa4021)
- Clement, M. S., Raymond, S. N., Kaib, N. A., et al. 2021, *Icarus*, 355, 114122, doi: [10.1016/j.icarus.2020.114122](https://doi.org/10.1016/j.icarus.2020.114122)
- Connerney, J. E. P., Acuna, M. H., & Ness, N. F. 1987, *J. Geophys. Res.*, 92, 15329, doi: [10.1029/JA092iA13p15329](https://doi.org/10.1029/JA092iA13p15329)
- Crida, A., & Charnoz, S. 2012, *Science*, 338, 1196, doi: [10.1126/science.1226477](https://doi.org/10.1126/science.1226477)
- Ćuk, M., El Moutamid, M., & Tiscareno, M. S. 2020, *PSJ*, 1, 22, doi: [10.3847/PSJ/ab9748](https://doi.org/10.3847/PSJ/ab9748)
- Ćuk, M., French, R. S., Showalter, M. R., Tiscareno, M. S., & El Moutamid, M. 2022, *AJ*, 164, 38, doi: [10.3847/1538-3881/ac745d](https://doi.org/10.3847/1538-3881/ac745d)
- Curtis, S. A., & Ness, N. F. 1985, *Geophys. Res. Lett.*, 12, 855, doi: [10.1029/GL012i012p00855](https://doi.org/10.1029/GL012i012p00855)
- Daisaka, H., Tanaka, H., & Ida, S. 2001, *Icarus*, 154, 296, doi: [10.1006/icar.2001.6716](https://doi.org/10.1006/icar.2001.6716)
- Dawson, R. I., & Murray-Clay, R. 2012, *ApJ*, 750, 43, doi: [10.1088/0004-637X/750/1/43](https://doi.org/10.1088/0004-637X/750/1/43)
- Deienno, R., Nesvorný, D., Vokrouhlický, D., & Yokoyama, T. 2014, *AJ*, 148, 25, doi: [10.1088/0004-6256/148/2/25](https://doi.org/10.1088/0004-6256/148/2/25)
- Deienno, R., Yokoyama, T., Nogueira, E. C., Callegari, N., & Santos, M. T. 2011, *A&A*, 536, A57, doi: [10.1051/0004-6361/201014862](https://doi.org/10.1051/0004-6361/201014862)
- Dermott, S. F., Malhotra, R., & Murray, C. D. 1988, *Icarus*, 76, 295, doi: [10.1016/0019-1035\(88\)90074-7](https://doi.org/10.1016/0019-1035(88)90074-7)
- Dermott, S. F., & Nicholson, P. D. 1986, *Nature*, 319, 115, doi: [10.1038/319115a0](https://doi.org/10.1038/319115a0)
- Dobos, V., Barr, A. C., & Kiss, L. L. 2019, *A&A*, 624, A2, doi: [10.1051/0004-6361/201834254](https://doi.org/10.1051/0004-6361/201834254)
- Elliot, J. L., Dunham, E., & Mink, D. 1977, *Nature*, 267, 328, doi: [10.1038/267328a0](https://doi.org/10.1038/267328a0)
- Esposito, L. W. 2002, *Reports on Progress in Physics*, 65, 1741, doi: [10.1088/0034-4885/65/12/201](https://doi.org/10.1088/0034-4885/65/12/201)
- Esposito, L. W., & Colwell, J. E. 1989, *Nature*, 339, 605, doi: [10.1038/339605a0](https://doi.org/10.1038/339605a0)
- Ferguson, S. N., Rhoden, A. R., & Kirchoff, M. R. 2020, *Journal of Geophysical Research (Planets)*, 125, e06400, doi: [10.1029/2020JE006400](https://doi.org/10.1029/2020JE006400)
- Fletcher, L. N., Simon, A. A., Hofstadter, M. D., et al. 2020a, *Philosophical Transactions of the Royal Society of London Series A*, 378, 20190473, doi: [10.1098/rsta.2019.0473](https://doi.org/10.1098/rsta.2019.0473)
- Fletcher, L. N., Helled, R., Roussos, E., et al. 2020b, *Planet. Space Sci.*, 191, 105030, doi: [10.1016/j.pss.2020.105030](https://doi.org/10.1016/j.pss.2020.105030)
- . 2022, *Experimental Astronomy*, 54, 1015, doi: [10.1007/s10686-021-09759-z](https://doi.org/10.1007/s10686-021-09759-z)
- Ford, E. B., & Chiang, E. I. 2007, *ApJ*, 661, 602, doi: [10.1086/513598](https://doi.org/10.1086/513598)
- French, R. G., Dawson, R. I., & Showalter, M. R. 2015, *AJ*, 149, 142, doi: [10.1088/0004-6256/149/4/142](https://doi.org/10.1088/0004-6256/149/4/142)
- French, R. S., & Showalter, M. R. 2012, *Icarus*, 220, 911, doi: [10.1016/j.icarus.2012.06.031](https://doi.org/10.1016/j.icarus.2012.06.031)
- Goldreich, P., & Porco, C. C. 1987, *AJ*, 93, 730, doi: [10.1086/114355](https://doi.org/10.1086/114355)
- Goldreich, P., & Tremaine, S. 1979, *Nature*, 277, 97, doi: [10.1038/277097a0](https://doi.org/10.1038/277097a0)
- Goldreich, P., & Tremaine, S. D. 1978, *Icarus*, 34, 227, doi: [10.1016/0019-1035\(78\)90164-1](https://doi.org/10.1016/0019-1035(78)90164-1)
- Greenberg, R. 1975a, *Icarus*, 24, 325, doi: [10.1016/0019-1035\(75\)90128-1](https://doi.org/10.1016/0019-1035(75)90128-1)
- . 1975b, *MNRAS*, 173, 121, doi: [10.1093/mnras/173.1.121](https://doi.org/10.1093/mnras/173.1.121)

- Hammond, N. P., & Barr, A. C. 2014, *Geology*, 42, 931, doi: [10.1130/G36124.1](https://doi.org/10.1130/G36124.1)
- Hedman, M. M., & Nicholson, P. D. 2013, *AJ*, 146, 12, doi: [10.1088/0004-6256/146/1/12](https://doi.org/10.1088/0004-6256/146/1/12)
- Helled, R., Anderson, J. D., & Schubert, G. 2010, *Icarus*, 210, 446, doi: [10.1016/j.icarus.2010.06.037](https://doi.org/10.1016/j.icarus.2010.06.037)
- Heller, R., Williams, D., Kipping, D., et al. 2014, *Astrobiology*, 14, 798, doi: [10.1089/ast.2014.1147](https://doi.org/10.1089/ast.2014.1147)
- Hill, M. L., Kane, S. R., Seperuelo Duarte, E., et al. 2018, *ApJ*, 860, 67, doi: [10.3847/1538-4357/aac384](https://doi.org/10.3847/1538-4357/aac384)
- Hinkel, N. R., & Kane, S. R. 2013, *ApJ*, 774, 27, doi: [10.1088/0004-637X/774/1/27](https://doi.org/10.1088/0004-637X/774/1/27)
- Horner, J., Vervoort, P., Kane, S. R., et al. 2020a, *AJ*, 159, 10, doi: [10.3847/1538-3881/ab5365](https://doi.org/10.3847/1538-3881/ab5365)
- Horner, J., Kane, S. R., Marshall, J. P., et al. 2020b, *PASP*, 132, 102001, doi: [10.1088/1538-3873/ab8eb9](https://doi.org/10.1088/1538-3873/ab8eb9)
- Hueso, R., Delcroix, M., Sánchez-Lavega, A., et al. 2018, *A&A*, 617, A68, doi: [10.1051/0004-6361/201832689](https://doi.org/10.1051/0004-6361/201832689)
- Hyodo, R., & Charnoz, S. 2017, *AJ*, 154, 34, doi: [10.3847/1538-3881/aa74c9](https://doi.org/10.3847/1538-3881/aa74c9)
- Hyodo, R., Charnoz, S., Ohtsuki, K., & Genda, H. 2017, *Icarus*, 282, 195, doi: [10.1016/j.icarus.2016.09.012](https://doi.org/10.1016/j.icarus.2016.09.012)
- Ida, S., Ueta, S., Sasaki, T., & Ishizawa, Y. 2020, *Nature Astronomy*, 4, 880, doi: [10.1038/s41550-020-1049-8](https://doi.org/10.1038/s41550-020-1049-8)
- Izidoro, A., Morbidelli, A., Raymond, S. N., Hersant, F., & Pierens, A. 2015, *A&A*, 582, A99, doi: [10.1051/0004-6361/201425525](https://doi.org/10.1051/0004-6361/201425525)
- Jacobson, R. A. 2014, *AJ*, 148, 76, doi: [10.1088/0004-6256/148/5/76](https://doi.org/10.1088/0004-6256/148/5/76)
- Johnson, T. V., Brown, R. H., & Pollack, J. B. 1987a, *J. Geophys. Res.*, 92, 14884, doi: [10.1029/JA092iA13p14884](https://doi.org/10.1029/JA092iA13p14884)
- Johnson, T. V., Brown, R. H., & Soderblom, L. A. 1987b, *Scientific American*, 256, 48, doi: [10.1038/scientificamerican0487-48](https://doi.org/10.1038/scientificamerican0487-48)
- Kane, S. R. 2011, *Icarus*, 214, 327, doi: [10.1016/j.icarus.2011.04.023](https://doi.org/10.1016/j.icarus.2011.04.023)
- . 2023, *PSJ*, 4, 38, doi: [10.3847/PSJ/acbb6b](https://doi.org/10.3847/PSJ/acbb6b)
- Kane, S. R., Hinkel, N. R., & Raymond, S. N. 2013, *AJ*, 146, 122, doi: [10.1088/0004-6256/146/5/122](https://doi.org/10.1088/0004-6256/146/5/122)
- Kane, S. R., & Li, Z. 2022, *PSJ*, 3, 179, doi: [10.3847/PSJ/ac7de6](https://doi.org/10.3847/PSJ/ac7de6)
- Kane, S. R., Arney, G. N., Byrne, P. K., et al. 2021, *Journal of Geophysical Research (Planets)*, 126, e06643, doi: [10.1002/jgre.v126.2](https://doi.org/10.1002/jgre.v126.2)
- Kegerreis, J. A., Teodoro, L. F. A., Eke, V. R., et al. 2018, *ApJ*, 861, 52, doi: [10.3847/1538-4357/aac725](https://doi.org/10.3847/1538-4357/aac725)
- Kenworthy, M. A., & Mamajek, E. E. 2015, *ApJ*, 800, 126, doi: [10.1088/0004-637X/800/2/126](https://doi.org/10.1088/0004-637X/800/2/126)
- Kipping, D. M., Forgan, D., Hartman, J., et al. 2013, *ApJ*, 777, 134, doi: [10.1088/0004-637X/777/2/134](https://doi.org/10.1088/0004-637X/777/2/134)
- Kirchoff, M. R., Dones, L., Singer, K., & Schenk, P. 2022, *PSJ*, 3, 42, doi: [10.3847/PSJ/ac42d7](https://doi.org/10.3847/PSJ/ac42d7)
- Kirchoff, M. R., & Schenk, P. 2010, *Icarus*, 206, 485, doi: [10.1016/j.icarus.2009.12.007](https://doi.org/10.1016/j.icarus.2009.12.007)
- Kobayashi, H., Watanabe, S.-i., Kimura, H., & Yamamoto, T. 2009, *Icarus*, 201, 395, doi: [10.1016/j.icarus.2009.01.002](https://doi.org/10.1016/j.icarus.2009.01.002)
- Korycansky, D. G., Bodenheimer, P., Cassen, P., & Pollack, J. B. 1990, *Icarus*, 84, 528, doi: [10.1016/0019-1035\(90\)90051-A](https://doi.org/10.1016/0019-1035(90)90051-A)
- Lainey, V. 2008, *Planet. Space Sci.*, 56, 1766, doi: [10.1016/j.pss.2008.02.015](https://doi.org/10.1016/j.pss.2008.02.015)
- Lane, A. L., West, R. A., Hord, C. W., et al. 1989, *Science*, 246, 1450, doi: [10.1126/science.246.4936.1450](https://doi.org/10.1126/science.246.4936.1450)
- Laskar, J. 1986, *A&A*, 166, 349
- . 1988, *A&A*, 198, 341
- Lazzaro, D. 1991, *A&A*, 250, 253
- Lazzaro, D., Ferraz-Mello, S., & Veillet, C. 1984, *A&A*, 140, 33
- Li, D., & Christou, A. A. 2020, *AJ*, 159, 184, doi: [10.3847/1538-3881/ab7cd5](https://doi.org/10.3847/1538-3881/ab7cd5)
- Li, D., Johansen, A., Mustill, A. J., Davies, M. B., & Christou, A. A. 2020, *A&A*, 638, A139, doi: [10.1051/0004-6361/201936672](https://doi.org/10.1051/0004-6361/201936672)
- Lithwick, Y., & Wu, Y. 2011, *ApJ*, 739, 31, doi: [10.1088/0004-637X/739/1/31](https://doi.org/10.1088/0004-637X/739/1/31)
- Lu, T., & Laughlin, G. 2022, *PSJ*, 3, 221, doi: [10.3847/PSJ/ac83c1](https://doi.org/10.3847/PSJ/ac83c1)
- Lunine, J. I., & Stevenson, D. J. 1982, *Icarus*, 52, 14, doi: [10.1016/0019-1035\(82\)90166-X](https://doi.org/10.1016/0019-1035(82)90166-X)
- Makarov, V. V., Berghea, C. T., & Efroimsky, M. 2018, *ApJ*, 857, 142, doi: [10.3847/1538-4357/aab845](https://doi.org/10.3847/1538-4357/aab845)
- Malhotra, R. 1991, *Icarus*, 94, 399, doi: [10.1016/0019-1035\(91\)90237-N](https://doi.org/10.1016/0019-1035(91)90237-N)
- Malhotra, R., Fox, K., Murray, C. D., & Nicholson, P. D. 1989, *A&A*, 221, 348
- Mankovich, C., Marley, M. S., Fortney, J. J., & Movshovitz, N. 2019, *ApJ*, 871, 1, doi: [10.3847/1538-4357/aaf798](https://doi.org/10.3847/1538-4357/aaf798)
- Mankovich, C. R., & Fuller, J. 2021, *Nature Astronomy*, 5, 1103, doi: [10.1038/s41550-021-01448-3](https://doi.org/10.1038/s41550-021-01448-3)
- Morbidelli, A., Tsiganis, K., Batygin, K., Crida, A., & Gomes, R. 2012, *Icarus*, 219, 737, doi: [10.1016/j.icarus.2012.03.025](https://doi.org/10.1016/j.icarus.2012.03.025)
- Nakajima, A., Ida, S., & Ishigaki, Y. 2020, *A&A*, 640, L15, doi: [10.1051/0004-6361/202038743](https://doi.org/10.1051/0004-6361/202038743)
- Ness, N. F., Acuna, M. H., Behannon, K. W., et al. 1986, *Science*, 233, 85, doi: [10.1126/science.233.4759.85](https://doi.org/10.1126/science.233.4759.85)

- Ogilvie, G. I. 2014, *ARA&A*, 52, 171,
doi: [10.1146/annurev-astro-081913-035941](https://doi.org/10.1146/annurev-astro-081913-035941)
- Paradis, S., Moeckel, C., & de Pater, I. 2023, *Icarus*, 391, 115331, doi: [10.1016/j.icarus.2022.115331](https://doi.org/10.1016/j.icarus.2022.115331)
- Parisi, M. G. 2011, *A&A*, 534, A28,
doi: [10.1051/0004-6361/201117085](https://doi.org/10.1051/0004-6361/201117085)
- Park, R. S., Folkner, W. M., Williams, J. G., & Boggs, D. H. 2021, *AJ*, 161, 105, doi: [10.3847/1538-3881/abd414](https://doi.org/10.3847/1538-3881/abd414)
- Peale, S. J. 1999, *ARA&A*, 37, 533,
doi: [10.1146/annurev.astro.37.1.533](https://doi.org/10.1146/annurev.astro.37.1.533)
- Peale, S. J., & Lee, M. H. 2002, *Science*, 298, 593,
doi: [10.1126/science.1076557](https://doi.org/10.1126/science.1076557)
- Petit, J. M., & Henon, M. 1988, *A&A*, 199, 343
- Plescia, J. B., & Boyce, J. M. 1985, *J. Geophys. Res.*, 90, 2029, doi: [10.1029/JB090iB02p02029](https://doi.org/10.1029/JB090iB02p02029)
- Pollack, J. B. 1975, *SSRv*, 18, 3, doi: [10.1007/BF00350197](https://doi.org/10.1007/BF00350197)
- Porco, C. C., & Goldreich, P. 1987, *AJ*, 93, 724,
doi: [10.1086/114354](https://doi.org/10.1086/114354)
- Porco, C. C., West, R. A., McEwen, A., et al. 2003, *Science*, 299, 1541, doi: [10.1126/science.1079462](https://doi.org/10.1126/science.1079462)
- Porco, C. C., Baker, E., Barbara, J., et al. 2005, *Science*, 307, 1226, doi: [10.1126/science.1108056](https://doi.org/10.1126/science.1108056)
- Quillen, A. C., & French, R. S. 2014, *MNRAS*, 445, 3959,
doi: [10.1093/mnras/stu2023](https://doi.org/10.1093/mnras/stu2023)
- Rein, H., & Liu, S. F. 2012, *A&A*, 537, A128,
doi: [10.1051/0004-6361/201118085](https://doi.org/10.1051/0004-6361/201118085)
- Rein, H., & Tamayo, D. 2015, *MNRAS*, 452, 376,
doi: [10.1093/mnras/stv1257](https://doi.org/10.1093/mnras/stv1257)
- Reinhardt, C., Chau, A., Stadel, J., & Helled, R. 2020, *MNRAS*, 492, 5336, doi: [10.1093/mnras/stz3271](https://doi.org/10.1093/mnras/stz3271)
- Ronnet, T., & Johansen, A. 2020, *A&A*, 633, A93,
doi: [10.1051/0004-6361/201936804](https://doi.org/10.1051/0004-6361/201936804)
- Rubincam, D. P. 2006, *Icarus*, 184, 532,
doi: [10.1016/j.icarus.2006.05.017](https://doi.org/10.1016/j.icarus.2006.05.017)
- Saillenfest, M., Rogoszinski, Z., Lari, G., et al. 2022, *A&A*, 668, A108, doi: [10.1051/0004-6361/202243953](https://doi.org/10.1051/0004-6361/202243953)
- Salmon, J., & Canup, R. M. 2017, *ApJ*, 836, 109,
doi: [10.3847/1538-4357/836/1/109](https://doi.org/10.3847/1538-4357/836/1/109)
- . 2022, *ApJ*, 924, 6, doi: [10.3847/1538-4357/ac300e](https://doi.org/10.3847/1538-4357/ac300e)
- Salo, H. 1995, *Icarus*, 117, 287, doi: [10.1006/icar.1995.1157](https://doi.org/10.1006/icar.1995.1157)
- Showalter, M. R. 2020, *Philosophical Transactions of the Royal Society of London Series A*, 378, 20190482,
doi: [10.1098/rsta.2019.0482](https://doi.org/10.1098/rsta.2019.0482)
- Showalter, M. R., Burns, J. A., Cuzzi, J. N., & Pollack, J. B. 1987, *Icarus*, 69, 458,
doi: [10.1016/0019-1035\(87\)90018-2](https://doi.org/10.1016/0019-1035(87)90018-2)
- Showalter, M. R., & Lissauer, J. J. 2006, *Science*, 311, 973,
doi: [10.1126/science.1122882](https://doi.org/10.1126/science.1122882)
- Slattery, W. L., Benz, W., & Cameron, A. G. W. 1992, *Icarus*, 99, 167, doi: [10.1016/0019-1035\(92\)90180-F](https://doi.org/10.1016/0019-1035(92)90180-F)
- Stanley, S., & Bloxham, J. 2006, *Icarus*, 184, 556,
doi: [10.1016/j.icarus.2006.05.005](https://doi.org/10.1016/j.icarus.2006.05.005)
- Sucerquia, M., Alvarado-Montes, J. A., Zuluaga, J. I., Montesinos, M., & Bayo, A. 2020, *MNRAS*, 496, L85,
doi: [10.1093/mnrasl/slaa080](https://doi.org/10.1093/mnrasl/slaa080)
- Thomas, P. C. 1988, *Icarus*, 73, 427,
doi: [10.1016/0019-1035\(88\)90054-1](https://doi.org/10.1016/0019-1035(88)90054-1)
- Tittemore, W. C., & Wisdom, J. 1988, *Icarus*, 74, 172,
doi: [10.1016/0019-1035\(88\)90038-3](https://doi.org/10.1016/0019-1035(88)90038-3)
- . 1989, *Icarus*, 78, 63, doi: [10.1016/0019-1035\(89\)90070-5](https://doi.org/10.1016/0019-1035(89)90070-5)
- . 1990, *Icarus*, 85, 394,
doi: [10.1016/0019-1035\(90\)90125-S](https://doi.org/10.1016/0019-1035(90)90125-S)
- Tyler, G. L., Sweetnam, D. N., Anderson, J. D., et al. 1986, *Science*, 233, 79, doi: [10.1126/science.233.4759.79](https://doi.org/10.1126/science.233.4759.79)
- Vervoort, P., Horner, J., Kane, S. R., Kirtland Turner, S., & Gilmore, J. B. 2022, *AJ*, 164, 130,
doi: [10.3847/1538-3881/ac87fd](https://doi.org/10.3847/1538-3881/ac87fd)
- Wakeford, H. R., & Dalba, P. A. 2020, *Philosophical Transactions of the Royal Society of London Series A*, 378, 20200054, doi: [10.1098/rsta.2020.0054](https://doi.org/10.1098/rsta.2020.0054)
- Woo, J. M. Y., Reinhardt, C., Cilibrasi, M., et al. 2022, *Icarus*, 375, 114842, doi: [10.1016/j.icarus.2021.114842](https://doi.org/10.1016/j.icarus.2021.114842)
- Zahnle, K., Schenk, P., Levison, H., & Dones, L. 2003, *Icarus*, 163, 263, doi: [10.1016/S0019-1035\(03\)00048-4](https://doi.org/10.1016/S0019-1035(03)00048-4)
- Zuluaga, J. I., Kipping, D. M., Sucerquia, M., & Alvarado, J. A. 2015, *ApJL*, 803, L14,
doi: [10.1088/2041-8205/803/1/L14](https://doi.org/10.1088/2041-8205/803/1/L14)